

Chitosan Depolymerization and Nanochitosan Production Using a Single Physical Procedure

Helton J. Alves^{1,4} · Mônica Vieceli¹ · Cássio Alves¹ · Graciela I. B. Muñiz² · Cristiano L. P. de Oliveira³ · Michael Feroldi¹ · Mabel K. Arantes¹

Published online: 16 June 2018
© Springer Science+Business Media, LLC, part of Springer Nature 2018

Abstract

The many applications of the chitosan biopolymers in the areas of nanotechnology and nanomaterials have led to the need to develop novel techniques suitable for the production of nanochitosan. At present these typically involve the use of chemical agents to form chitosan nanoparticles. Physical, chemical, and enzymatic methods have been described for the depolymerization of chitosan. In this work, evaluation was made of the efficiency of a combination of physical methods, including milling of the raw material and drying of the final chitosan, in order to obtain nanochitosan with low molar mass. The results revealed the effectiveness of the combination of milling the raw material under controlled conditions for 4.5 h and drying of the chitosan by thermal shock, which provided depolymerization of up to 10× and resulted in chitosan with M_v less than 21 kDa and hydrodynamic diameter below 30 nm.

Keywords Biopolymers · Chitosan · Depolymerization · Milling · Drying · Nanomaterials

Introduction

Chitosan, a polysaccharide usually produced by the deacetylation of chitin, has a molar mass that generally lies between 10 and 10^3 kDa, depending on the source from which it is extracted and the physical and chemical processes used in the processing of chitin to form chitosan. These processes include preparation of the raw material, the extraction and deacetylation of chitin, and the drying stage [1, 2]. There have been many studies concerning techniques employed to obtain chitosan, as well as its uses, considering various aspects of this material, including its biological activity,

biodegradability, toxicity, and antimicrobial activity [2–4]. It possesses valuable properties for uses in the areas of nanotechnology and nanomaterials [5–7], and can be chemically modified to produce various functionalities [8, 9].

Chitosan nanomaterials have important uses in the areas of nanomedicine, pharmaceuticals, nutraceuticals, food, and the environment. In different size ranges, nanochitosan has applications in medicine (200–500 nm), microbiology (70–400 nm), the production of modified nanoparticles (NPs) such as chitosan NPs-carboxymethyl cellulose (8–110 nm) [5], the removal of $\text{Cr}^{(n+)}$ (100–400 nm) [10] and Cadmium (34.6 nm) [11] and as flocculants agents for harvesting microalga (13.7 nm) [12], among others. Various techniques have been described for the production of chitosan NPs, including use of a multifunctional crosslinking agent in a chitosan emulsion, coacervation/precipitation using alkaline or organic solutions, emulsion-droplet coalescence, and ionotropic gelation with cross-linking using sodium tripolyphosphate (TPP) [13]. The last method has been used to obtain nanochitosan with sizes 100–400 nm [10], 130–196 nm [14], and < 500 nm [15].

Many applications require nanochitosan with low molar mass, which can be obtained using depolymerization techniques. Methods for the controlled depolymerization of chitosan include milling of the raw materials [16], the use

✉ Helton J. Alves
helquimica@gmail.com

¹ Department of Engineering and Exact, Federal University of Paraná - UFPR, Rua Pioneiro 2153, Jardim Dallas, Palotina, PR 85950-000, Brazil

² Department of Forest Engineering and Technology, Federal University of Paraná, Av. Pref. Lothario Meissner, 900, Jardim Botânico, Curitiba, PR 80210-170, Brazil

³ Institute of Physics, University of São Paulo, Rua do Matão 1371, São Paulo, SP 05508-090, Brazil

⁴ Rua Pioneiro, 2153, Jd Dallas, Palotina, PR 85950-000, Brazil

of ultrasound during chitin deacetylation [17] or applied to chitosan solutions [18], degradation induced by an electron beam plasma [19], autoclaving of chitosan solutions [20, 21], gamma irradiation [22], and drying procedures [1]. Enzymatic and chemical methods include the use of non-specific enzymes [23, 24], chitinase [25], strong acid [26] or hydrogen peroxide [27]. In the case of the enzymatic methods, obstacles include high costs, the need to control the experimental conditions in order to maintain the enzymatic activity, long treatment times, and the need for additional steps to separate and purify the chitosan (these steps are also required in the case of chemical methods).

Advances in processes for the depolymerization of chitosan enable the production of oligomers and molecular structures at the nanoscale (nanochitosan). Especially attractive are physical methods that provide fast depolymerization of the material, without the need for additional purification steps. One such technique is milling the raw material (shrimp shells) in order to reduce the viscosimetric molar mass (M_v) of the chitosan produced. Results obtained by our research group [16] showed that an increase of the milling time from 30 to 180 min decreased the M_v of depolymerized chitosan by approximately fourfold, from 502 to 131 kDa. Other previous work by the same group [1] showed the effect of drying on the molar mass of chitosan, with better results being achieved by drying with supercritical CO_2 ($M_v = 3$ kDa), compared to oven drying ($M_v = 17$ kDa). Decreases of M_v of around 10-fold and twofold were obtained, respectively, relative to the initial sample.

The results obtained in these studies indicated the potential of the combination of milling the initial raw material and oven-drying the final chitosan as a way to obtain a highly depolymerized nanometric-scale biopolymer, simply by controlling the physical processes. This offers the convenience of obtaining, in a single process, a low molar mass nanomaterial with desirable characteristics for various applications. In the present work, different combinations of conditions for milling the raw material and drying the chitosan were compared to autoclaving, considering the depolymerization efficiency and the formation of nanochitosan.

Materials and Methods

Methodologies for obtaining chitosan from shrimp shells and depolymerizing it via Method III (see Sect. 2.2) are protected by patent application number BR 102017022250 [28].

Procedures for Obtaining Chitin and Chitosan

Saltwater shrimp shells, an aquaculture waste, were washed under running water and dried at 60 °C, after which they were crushed to a particle size smaller than 1 mm, ground

in a ball mill for periods of 4.5 (sample A) and 6 h (sample B), and passed through a 63 µm (230 mesh) sieve. Chitin was extracted by demineralization with 0.55 mol L⁻¹ HCl solution (three washes of 15 min each), under agitation, followed by deproteinization with 0.3 mol L⁻¹ NaOH solution at 80 °C, under stirring (three washes of 20 min each). After these steps, the material was washed to neutralize the pH, followed by deacetylation of the chitin by mixing it (in a proportion of 6.7%) with a solution of NaOH (70% w/v) and agitating for 14 days in a rotary incubator at 125 rpm. The reaction product was washed to neutralize the pH, followed by depolymerization of the chitosan (as described in Sect. 2.2). Sample C was a commercial chitosan (obtained from Sigma-Aldrich) of medium molar mass, viscosity of 200–800 cps, and degree of deacetylation of 75–85% (as stated on the product data sheet).

Techniques for Chitosan Depolymerization

Chitosan samples A, B, and C were submitted to different physical processes for depolymerization of the biopolymer chains, as described in Fig. 1. It should be noted that samples A and B used in depolymerization Method I had not been dried after the neutralization washing step performed after chitin deacetylation.

Depolymerization Method I (Drying at Ambient Temperature and Autoclaving)

Chitosan obtained after deacetylation and neutralization was used as a reference (denoted R). This material had been dried in Petri dishes under ambient conditions for 6 days, in order to avoid depolymerization associated with the drying step. It should be noted that drying under ambient conditions was not used as a depolymerization method, but instead as a control (or as a reference). The samples obtained after the drying period were denoted A-R and B-R. This procedure was not used for the commercial sample (C-R), because the material was already dry.

The chitosan samples were solubilized at a concentration of 0.73 mg mL⁻¹ in a 1:1 mixture of HAc (0.3 M) and NaOAc (0.2 M), which provided suitable conditions for viscosimetric analysis. The samples were then autoclaved at 121 °C and 1 atm for 5 min [20, 21], cooled, and then immediately submitted to viscosimetric molar mass analysis. The resulting chitosan samples were denoted A-I, B-I, and C-I.

Depolymerization Method II (Autoclaving and Thermal Shock Drying)

Samples A, B, and C were solubilized and autoclaved, as described for Method I. Chitosan particles were then obtained by precipitation with 2 M NaOH, followed by

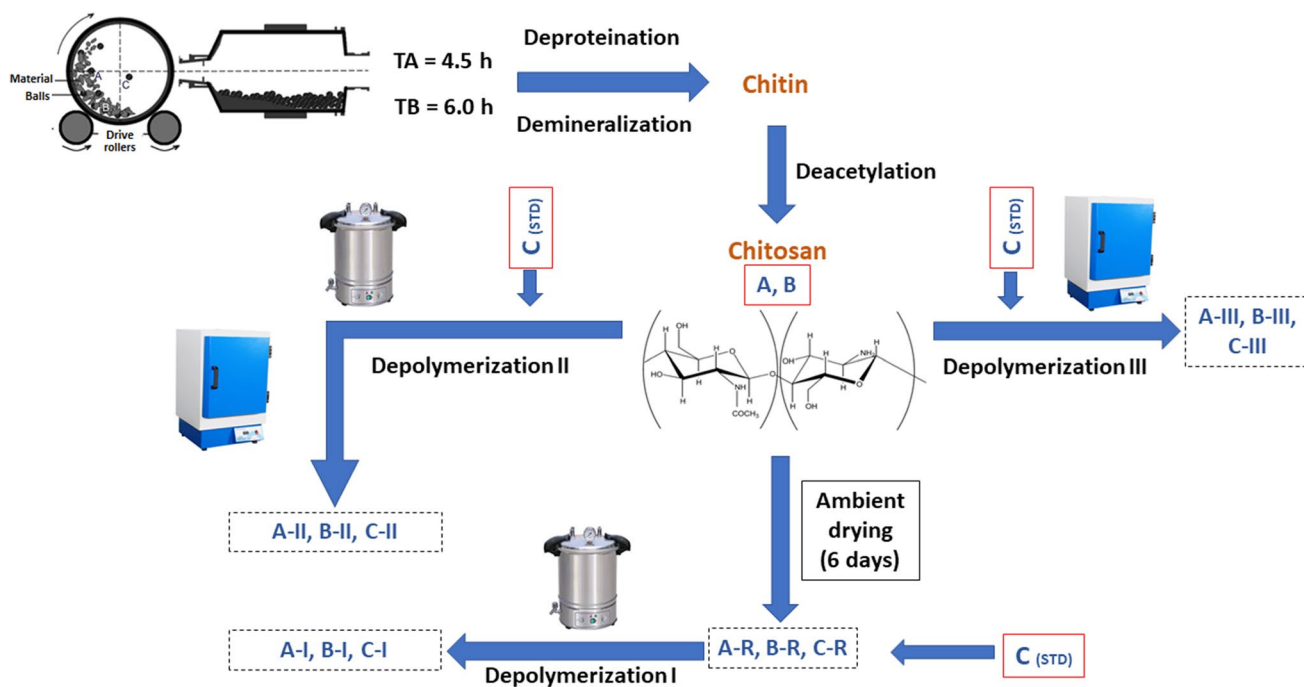


Fig. 1 Scheme of experiments used to evaluate different methods for depolymerization of chitosan

washing to neutral pH and filtering. The material was transferred to Petri dishes, in thin layers (~ 2 mm), for thermal shock drying using cycles of 5 min at 100°C (in an oven) and 5 min at room temperature, during 3 h. The material was then removed with a spatula and triturated in a mortar until it passed through a $63\text{ }\mu\text{m}$ sieve (230 mesh). The chitosan samples obtained after this process were denoted A-II, B-II, and C-II.

Depolymerization Method III (Thermal Shock Drying)

Samples A, B, and C were solubilized as described for Method I, followed by drying using thermal shock, as described for Method II. The resulting chitosan samples were denoted A-III, B-III, and C-III.

Physicochemical Characterization of Chitosan

Viscosimetric Molar Mass

The type R chitosan samples resulting from processing using Methods II and III were in a final dry form. The viscosimetry was performed using solutions with chitosan concentrations between 0.31 and 0.73 mg mL^{-1} (in $0.3\text{ M HAc}/0.2\text{ M NaOAc}$), with eight points. The sample treated using Method I had been autoclaved at a concentration of 0.73 mg mL^{-1} in the HAc/NaOAc solution, so it only required dilutions down to 0.31 mg mL^{-1} . The intrinsic viscosities of the solutions were obtained using an Ubbelohde dilution viscosimeter (Cannon

instrument Co., USA) fitted with a 0.44 mm capillary, in a water bath at 25°C . The relation between the intrinsic viscosity, $[\eta]$, and the mean viscosimetric molar mass of the polymer, M_V , was obtained using the Mark-Houwink-Sakurada equation: $([\eta] = K M_V^{\alpha})$ where K and α are constants for a given polymer–solvent system, which in the case of chitosan varies according to the degree of acetylation (DA) [29].

Degree of Deacetylation (DD)

The DD of the chitosan produced in the laboratory by the deacetylation process (samples A and B) was evaluated by conductimetric titration of acid solutions of chitosan with NaOH solution, as described by Santos et al. [30]. The DD of commercial sample C was provided by the manufacturer.

Absolute Density and Particle Size Distribution (PSD)

The absolute densities of chitosan samples A, B, and C were determined by helium gas pycnometry (Ultrapycnometer 1000, Quantachrome). The samples were submitted to X-ray sedimentometry assays (Sedigraph 5000 D, Micromeritics) to obtain the PSD curves.

Hydrodynamic Diameter Determination by Dynamic Light Scattering (DLS)

The DLS measurements were performed in triplicate, at 25°C , using a 90Plus Particle Size Analyzer (Brookhaven

Instruments), at a wavelength of 657 nm and with the detector perpendicular to the incident beam. After the depolymerization processes (Methods I, II, and III), DLS experiments were performed to determine the diameters of samples A and B.

Analyses were performed using photon correlation spectroscopy, with calculation of the time correlation function to fit the data (Eq. 1) [31, 32]. This application used the sum of the exponentials as the time correlation function (Eq. 2).

$$C(\tau) = \langle I(t)I(t + \tau) \rangle = \lim_{N \rightarrow \infty} \frac{1}{N} \sum_j^N I_j I_{j+n} \quad (1)$$

$$C(\tau) = \sum_{n=1}^N A_n \exp(-\Gamma_n \tau) \quad (2)$$

A_n is the intensity-weighted value proportional to the fraction of the scattered intensity, $\Gamma = q^2 D_i$ is the reciprocal decay time, D is the translational self-diffusion coefficient of the particle, and q is the scattering vector length ($q = (4\pi/\lambda) \sin(\theta/2)$) [32].

The correlation function data were fitted using the CONTIN algorithm, which fits an exponential distribution function.

Results and Discussion

Chitosan Particle Size Distribution (PSD)

The PSD curves for chitosan samples A, B, and C were obtained by X-ray sedimentometry and are shown in Fig. 2.

In Fig. 2, it can be seen that the PSD curve for sample B presented the greatest slope, in the particle diameter range considered, which when compared to the results of sample A could be attributed to the presence of finer particles, especially above 1.2 μm . Below this diameter, the particles of the two samples showed similar size distributions. Therefore, it appeared that the longer shrimp shell milling time used for sample B (6.0 h) led to a smaller mean diameter of the chitosan particles, compared to sample A (milled for 4.5 h). This was confirmed by the values obtained for D_{50} (Table 1), which is a statistical parameter extracted from PSD curves, representing the average particle diameter at a cumulative mass of 50%. Therefore, the lower D_{50} value for sample B (1.3 μm) indicated that the PSD curve shifted to the left, relative to the curve for sample A (1.5 μm), which was associated with more effective milling of the material, resulting in finer particles. This trend was observed in previous work by our group [16], using the same type of shrimp shells and the same conditions employed in the present work, with milling

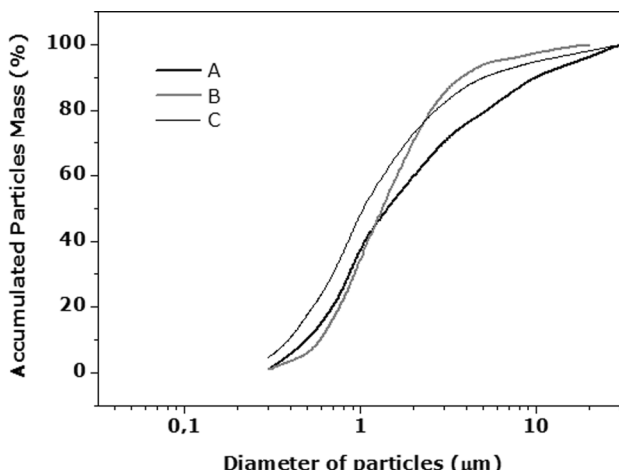


Fig. 2 Particle size distributions of chitosan samples A, B, and C

for times of 0.5 and 3.0 h resulting in chitosan D_{50} values of 2.5 and 1.7 μm , respectively (a comparison of the values is provided in Table 1, highlighting sample M5).

Below a diameter of 2.3 μm , the commercial sample (C) showed particles smaller than those in samples A and B (with the curve being shifted further to the left in Fig. 2). Above this value, the size distribution was similar to that of sample B, resulting in a D_{50} value of 1.0 μm .

The X-ray sedimentometry technique is limited to accurate measurements of particles with mean diameters above 300 nm. However, for the samples analyzed, the percentages of chitosan particles with diameters smaller than 300 nm were negligible.

It is expected that the higher the cumulative mass percentage of chitosan particles with small diameters (low D_{50} values), the more likely the material will be to undergo depolymerization, producing NPs.

Effect of Deacetylation Method on DD and M_v

Chitosan samples A and B, obtained by deacetylation in the laboratory, presented DD values in the ranges 65–67% and 54–57%, respectively. The commercial chitosan (sample C) had a declared DD of 75–85%. In this work, deacetylation was performed at ambient temperature and pressure, hence simplifying the process, because there was no need for refluxing at temperatures above 100 °C (which is employed in conventional chitosan production processes). The use of heat leads to chitosan with low molar mass (35 kDa) and high DD (96–97%), as found in previous work of our group [1]. Under the ambient conditions employed in the present work, the biopolymers obtained had sizes between 71 and 111 kDa and DD between 54 and 67% (Table 1). These values were in agreement with previous results obtained using the same production conditions, but with deacetylation for 7

Table 1 Shrimp shell milling conditions and physicochemical properties of chitosan samples A, B, and C, dried under ambient conditions (R) and after the depolymerization processes

Sample	Shrimp shell		Chitosan					M_v ^d (kDa) depolymerization
	Milling parameters		Particles D50 (μm) ^c	Deacetylation DD (%)	Viscosity ^a [η] (mL g ⁻¹)			
	Time (h)	Spheres ^b 20 mm (% wt)			R	I	II	III
M5*	3.0	100	1.7	78	589±10	131*		
A	4.5	100	1.5	65–67	369±5	71	48	29
B	6.0	100	1.3	54–57	527±2	113	72	18
C	**	100	1.0	75	518±2	111	62	20
								6

*Previous work employing the same conditions [16]

**Commercial chitosan

***The viscosimetric method employed did not allow determination of M_v below 3.0 kDa

^aK=0.074 and α =0.76 (solvent 0.3 M HAc/0.2 M NaAc, at 25 °C) [29]

^bThe total loading of balls was 1390±2.0 g

^cAn absolute density value of 1.5454 g cm⁻³ was determined by helium pycnometry and used in the X-ray sedimentometry

^dCalculation of M_v used the average value of [η]

days, where the M_v values were between 131 and 217 kDa, and DD was between 77 and 80% [16]. This indicated that deacetylation under ambient conditions resulted in lower depolymerization of chitosan. Despite the lower deacetylation efficiency, this would not prohibit the use of the material in applications that do not require a very high DD.

Effects of Milling, Drying, and Autoclaving on Depolymerization

The efficiencies of the depolymerization processes were evaluated by determination of the viscosimetric molar masses (M_v) of the chitosan samples before and after the procedures. The shrimp shell milling times selected here (4.5 and 6 h) were based on the effects observed previously for depolymerization by milling for times between 30 min and 3 h, where greater depolymerization of the chitosan (to 131 kDa) was obtained with 3 h of milling (sample M5 in Table 1) [16]. In the present work, no further decrease in molar mass was observed with milling for longer than 4.5 h.

The M_v values obtained before and after the processes (Table 1), together with the M_v profiles (Fig. 3), demonstrated the reproducibility of the depolymerization processes for the three sample types (A, B, and C). The use of autoclaving alone (Method I) resulted in depolymerization of the chitosan solution, as found in other studies [20, 21], but showed the lowest efficiency among the three methods. The combination of autoclaving and oven-drying (Method II) led to greater depolymerization and lower M_v . However, the best result, in terms of reduction of M_v , was obtained when drying was performed in intermittent mode, delivering thermal shocks to the material (Method III). Depolymerization by

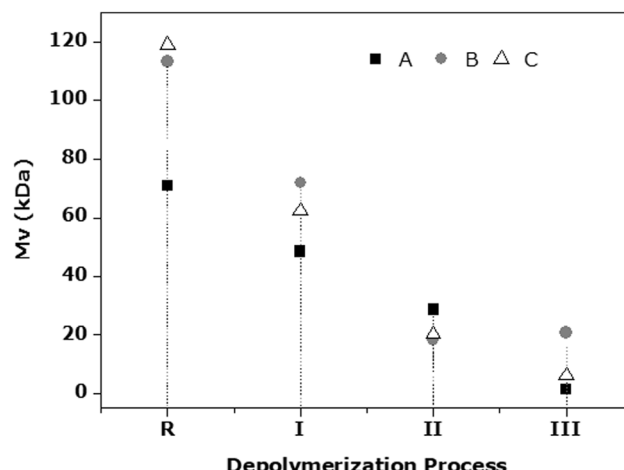


Fig. 3 Molar masses of chitosan samples A, B, and C, dried under ambient conditions (R), and of the materials obtained after treatment using depolymerization methods I, II, and III

oven-drying with thermal shock was previously attributed to an increase in the thermal vibration and disruption of C–C bonds in the polymer main chain [1].

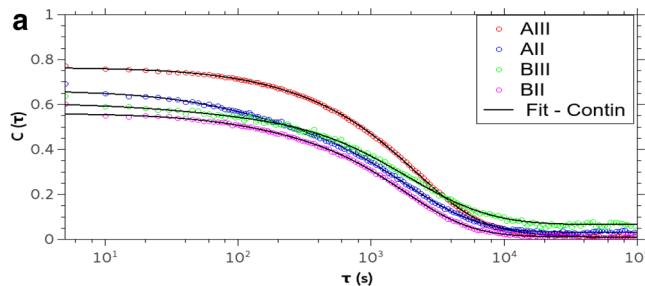
The results showed that it was possible to obtain a high degree of depolymerization of chitosan using two physical techniques to prepare the raw material: milling the shrimp shells and drying the deacetylated chitosan in an oven, with thermal shock. The use of these techniques, without the need for chemical agents, enzymes, or radiation, resulted in depolymerization that was comparable to that obtained previously for chitosan dried using supercritical CO₂, where chitosan with M_v of 3.0 kDa was produced.

When comparing results of this study with results obtained via other chitosan depolymerization methods (Table 2), it is noteworthy that both physical methods, such as gamma rays, ultrasound, ultra-fine milling and pulsed electric fields, as well as chemical methods, such as oxidative degradation and acid hydrolysis, show high depolymerization rates. In assessing these methods several characteristics and issues were reported by researchers: high molar mass chitosan has higher sensitivity to depolymerization; chemical methods lead to the common problem of purifying and separating chitosan from the employed chemical reagents; when employing either radiation or acids there are reports of chitosan degradation, sometimes causing the material to change color; high energy consumption is inevitable when employing physical methods, while chemical methods struggle with cost and residues generation issues. Also, some of the techniques shown in Table 2, although successful in obtaining reduction and depolymerization, were unable to obtain low molar masses.

Although the method employed in this study shares with others the consumption of energy to produce thermal shock, it has the advantage of eliminating the separation and purification step, and of employing diluted solutions in advance of thermal shock. Techniques employed in this research can be considered advantageous in comparison to several of the methods described in the literature, especially in terms of simplicity of the experimental apparatus and optimization of the chitosan milling and drying process, with no additional material processing steps required.

Table 2 Number distribution size of hydrodynamics diameter

Samples	D (nm)	Fit-method
BIII	1–4	Contin
AII	7–12	Contin
BII	15	Contin
AIII	28	Contin



Production of Nanochitosan

Results of DLS Analyses

The average hydrodynamic diameter was determined using the number size distribution (Fig. 4).

This type of normalized distribution presents the relative number distribution of different diameter particles present in the solution. Analyses of nanochitosan formation were performed using samples A and B treated using Methods II (autoclaving followed by oven drying) and III (oven drying in one step), since these techniques provided the best depolymerization (Table 1; Fig. 3). The hydrodynamic diameters were smallest for B-III (1–4 nm), followed by A-II (7–12 nm) (Table 3). The highest values were obtained for A-III (28 nm) and B-II (15 nm). Figure 4 shows the time correlation function data and the corresponding fitted curve, together with the number size distribution. The distribution values normalized by volume and intensity were dispersed in two groups (Fig. 5), one with sizes of around several dozens of nanometers and the other with sizes in the region of 3 μm. The number size distribution was concentrated in the larger size group. These results indicated that there were few particles with large hydrodynamic diameters (in the micrometer region) and that the larger particles scattered most of the light and did not represent the total population of particles present in the samples. The majority of the particles presented sizes smaller than 30 nm (Fig. 4), in the size range where the number distribution showed high precision.

Depolymerization Method III produced chitosan with smaller molar mass, compared to Method II, as confirmed by DLS analyses of the B samples, which showed a smaller hydrodynamic diameter of chitosan produced using Method III. The two methods showed similar results for the A samples. These findings indicated that the chitosan produced using Method II had a larger polymer chain but a smaller (or similar) hydrodynamic diameter, compared to the Method III material, because the chain was hydrophobic and was folded into a smaller volume.

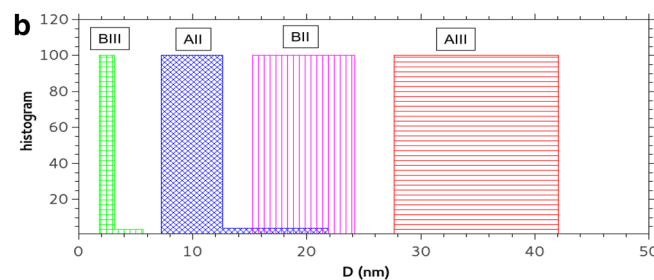


Fig. 4 **a** Time correlation functions and the corresponding fitted curves, using the CONTIN method applied to samples A-II, A-III, B-II, and B-III. **b** Histograms of particle number distribution according to hydrodynamic diameter

Table 3 Summary of studies on chitosan depolymerization processes (best results)

Reference	Depolymerization method	Temperature (°C)	Time (h)	Deacetylation DD (%)	Initial M_v (kDa)	Final M_v (kDa)	Notes
This work	Ball milling ^a and drying	Ball milling ^a : Room + thermal shock drying; 100	4.5 + 3.0	65–67	71	3–21	Optimized method, does not modify any processing steps; modifies milling and final drying operating conditions; obtains nanochitosan; higher energy consumption when milling and drying
[33]	Oxidative degradation with NaNO ₂ (0.1 M)	Room	3	83–85	600	5–100	Difficulties in separation and purification
[34]	Irradiation by Co-60 gamma rays (200 kGy)	Room	^b	^b	61 and 110	^c	Darkening of the chitosan solution due to cleavage of the structure and formation of double bonds above 100 kGy; energy consumption
[35]	Phosphoric acid (85%)	60	15	96	214	19	Strong and highly-concentrated acid; residue generation; requires separation and purification
[36]	Ultrasound (360 kHz; nominal power 100 W; dose rate 170 W kg ⁻¹ ; Ar-saturated aqueous solution at pH 3.0, HClO ₄)	22	6	88	323	≈40	Cleavage is followed by secondary reactions leading to formation of carbonyl groups; energy consumption; strong oxidizing agent
[37]	Acetic acid hydrolysis (5% v/v)	50	24	75	1360	88	Produces hydrogels; acid consumption; prolonged duration
[38]	Ultra-fine milling—dry (high-energy nano-ball-mill/ZrO ₂ balls)	30	12	^b	767 66	361 54	Average particle size between 35.5 and 375.2 nm; distribution volume with low contribution below the 100 nm level; high energy consumption during milling
[39]	Irradiation by Co-60 gamma rays (100 kGy)	Room	^b	92	577	106	Darkening of the chitosan solution due to cleavage at 100 kGy; complex equipment apparatus/energy consumption
[40]	Ultrasound (20 kHz; nominal power 95 W)	25	0.5	80	2099	450	Unable to obtain low molar masses; energy consumption
[41]	Pulsed electric fields (PEF) (25 kV cm ⁻¹ ; 1000 Hz)	50	^d	95	281	154	Unable to obtain low molar masses; energy consumption

Table 3 (continued)

Reference	Depolymerization method	Temperature (°C)	Time (h)	Deacetylation DD (%)	Initial M_v (kDa)	Final M_v (kDa)	Notes
[42]	Ball-milling (ZrO_2 balls)	30	10	92	809	108	New C=O groups might be formed during the milling process; crystalline structure of chitosan destroyed, resulting in darkening of the chitosan powder; prolonged milling duration; energy consumption
[43]	Dry heat and Saturated Steam	Oven: 120 Anoxia: 120 Autoclave: 115	4 4 2	95–99	≈ 1200 ^c ≈ 1320 ^c ≈ 1200 ^c	≈ 1030 ^e ≈ 1160 ^e ≈ 560 ^e	Darkening of the chitosan with increased drying temperatures; autoclave requires pressure and energy consumption; additional treatments are inefficient
[44]	Deacetylation temperature (NaOH 50%)	99 140	9 9	92.2 99.1	5637 ^f	182 63	Depolymerization occurs with increased temperature and deacetylation time
[45]	Sequential enzyme treatment by chitinase and chitin deacetylase	42	0.66	81.8	^b	4.7	pH influences enzymatic action; DD and M_v in inverse relationship ($M_v \uparrow DD$); initial M_v not reported

^aShrimp shell milling duration (not an additional step, but rather an increment to conventional milling)

^bNot assessed or reported

^cNinety-five percent (95%) reduction in viscosity for the two assessed chitosan products, wherein around 92% of the chitosan became water-soluble

^dTwelve pulses, each 20 μ s in duration

^eValues pertaining intrinsic viscosity; M_v not reported

^fMolar mass for chitin (the study focused on deacetylation)

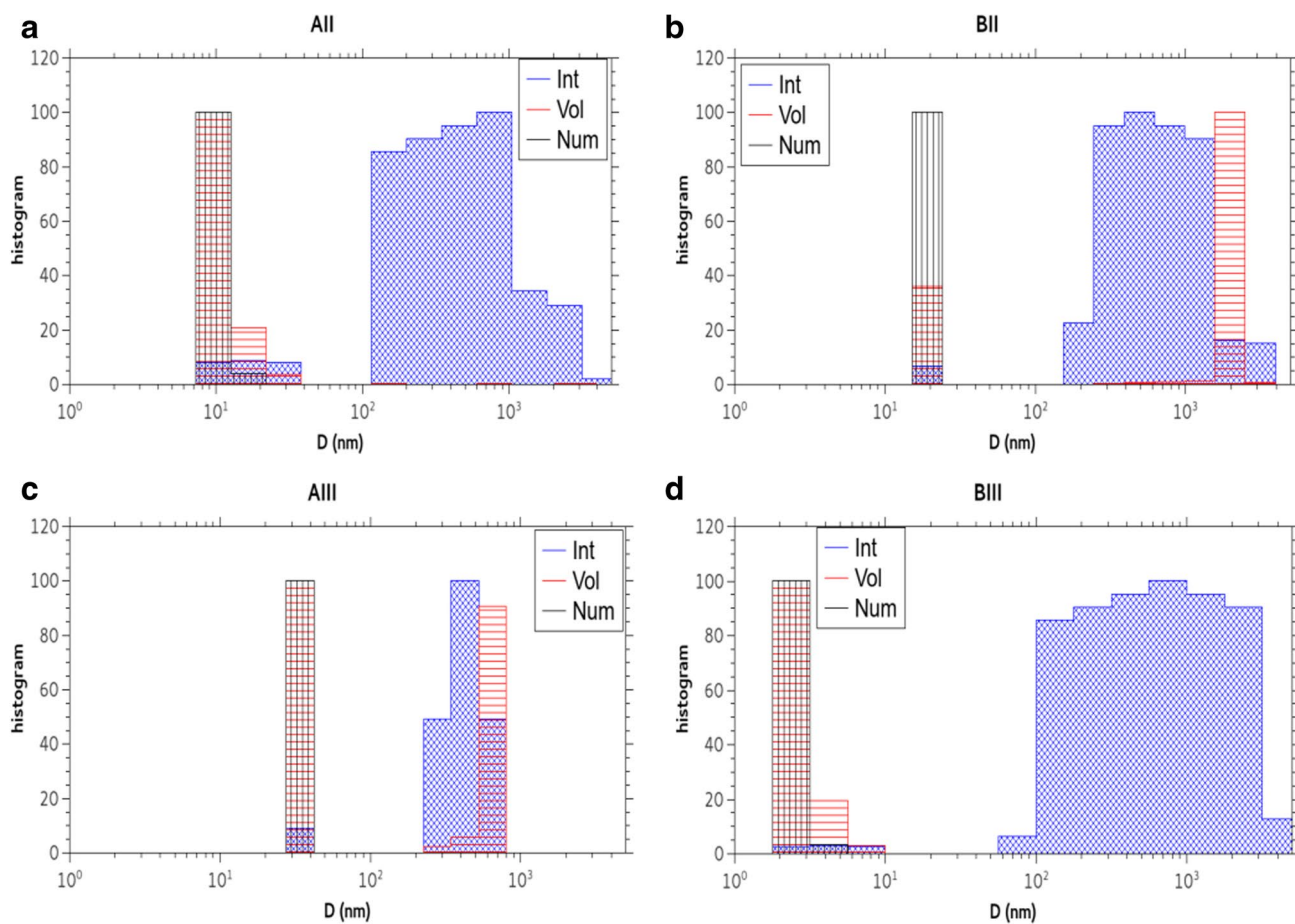


Fig. 5 Particle number, volume, and intensity distributions, according to hydrodynamic diameter, for samples **a** A-II, **b** A-III, **c** B-II, and **d** B-III

The differences between the PSD curves (Fig. 2) of chitosans A and B, where B generally showed finer particles than A (due to the more effective milling), did not reflect greater depolymerization of B, compared to A, as evaluated by viscosimetry (Table 1). However, the smaller average particle size of chitosan B could have contributed to the smaller size of the chitosan NPs produced by Method III, as measured by DLS. Hence, the diameter distribution of the B-III nanoparticles, which was concentrated between 1 and 4 nm (Figs. 4, 5), was probably the result of the combined effects of the use of finer particles of chitosan obtained by more effective milling, together with the efficiency of depolymerization Method III.

Final Considerations

As reported in the literature, the depolymerization of chitosan and production of chitosan NPs can be achieved by separately applying methodologies to reduce the molar mass of chitosan and to produce NPs of this biopolymer. The techniques most commonly described for obtaining NPs of low,

medium, or high molar mass include ionotropic gelation with TPP [10, 14, 15] or emulsion crosslinking, coacervation/precipitation, and emulsion-droplet coalescence techniques [13].

The most important contribution of the present study is that the same set of methodologies could be used to achieve depolymerization of chitosan, as well as to produce material at the nanometric scale (nanochitosan). There are potential applications for a biopolymer that is nanometric in size and that also has a very low molar mass (such as depolymerized chitosan). In addition, the process described here offers a way to avoid problems reported in the pharmaceutical literature, such as the loss of drugs during NPs preparation, or sensitivity to changes in pH and ionic strength that could lead to aggregation and precipitation of the material.

An especially interesting aspect of the methodology developed in this work is its relative simplicity, since it involves the physical processes of milling the raw material and drying the final product, which are already employed in the processing of shrimp shells to obtain chitosan. In this

work, these processes were optimized in order to obtain nanochitosan with low molar mass.

Conclusions

The findings demonstrated that the combination of milling shrimp shells under controlled conditions and drying chitosan by thermal shock provided more effective depolymerization and reduction of the material to the nanometric scale, compared to the autoclaving technique (used alone or in combination with drying). The proposed physical procedure could replace processing steps described in the literature for achieving depolymerization and/or production of nanoscale chitosan particles, allowing nanochitosan with low molar mass to be obtained in a single procedure. The technique enabled efficient and reproducible formation of nanochitosan with hydrodynamic diameter below 30 nm and molar mass between 3 and 21 kDa.

References

- Arantes MK, Kugelmeier CL, Cardozo-Filho L et al (2014) Influence of the drying route on the depolymerization and properties of chitosan. *Polym Eng Sci* 55:1969–1976. <https://doi.org/10.1002/pen>
- Muanprasat C, Chatsudhipong V (2017) Chitosan oligosaccharide: biological activities and potential therapeutic applications. *Pharmacol Ther* 170:80–97. <https://doi.org/10.1016/j.pharmthera.2016.10.013>
- Kaya M, Asan-Ozusaglam M, Erdogan S (2016) Comparison of antimicrobial activities of newly obtained low molecular weight scorpion chitosan and medium molecular weight commercial chitosan. *J Biosci Bioeng* 121:678–684. <https://doi.org/10.1016/j.jbiosc.2015.11.005>
- Tan W, Zhang J, Luan F et al (2017) Design, synthesis of novel chitosan derivatives bearing quaternary phosphonium salts and evaluation of antifungal activity. *Int J Biol Macromol* 102:704–711. <https://doi.org/10.1016/j.ijbiomac.2017.04.073>
- Gopal GRY, Nandakumar KSLC. (2015) Chitosan nanoparticles for generating novel systems for better applications: a review. *J Mol Genet Med* s4:005. <https://doi.org/10.4172/1747-0862.S4-005>
- Elgadir MA, Uddin MS, Ferdosh S et al (2015) Impact of chitosan composites and chitosan nanoparticle composites on various drug delivery systems: a review. *J Food Drug Anal* 23:619–629. <https://doi.org/10.1016/j.jfda.2014.10.008>
- Mura S, Corriás F, Stara G et al (2011) Innovative composite films of chitosan, methylcellulose, and nanoparticles. *J Food Sci* 76:54–60. <https://doi.org/10.1111/j.1750-3841.2011.02295.x>
- Gupta VK, Fakhri A, Agarwal S, Azad M (2017) Synthesis and characterization of Ag2S decorated chitosan nanocomposites and chitosan nanofibers for removal of Lincosamides antibiotic. *Int J Biol Macromol* 103:1–7. <https://doi.org/10.1016/j.ijbiomac.2017.05.018>
- Tamer TM, Hassan MA, Omer AM et al (2017) Antibacterial and antioxidative activity of O-amine functionalized chitosan. *Carbohydr Polym* 169:441–450. <https://doi.org/10.1016/j.carbpol.2017.04.027>
- Sivakami MS, Gomathi T, Venkatesan J et al (2013) Preparation and characterization of nano chitosan for treatment wastewaters. *Int J Biol Macromol* 57:204–212. <https://doi.org/10.1016/j.ijbiomac.2013.03.005>
- Seyed SM, Anvaripour B, Motavassel M, Jadidi N (2013) Comparative cadmium adsorption from water by nanochitosan and chitosan. *Int J Eng Innov Technol* 5:145–148
- Farid MS, Shariati A, Badakhshan A, Anvaripour B (2013) Using nano-chitosan for harvesting microalgae *Nannochloropsis* sp. *Bioresour Technol* 131:555–559. <https://doi.org/10.1016/j.biortech.2013.01.058>
- Davis SP (2011) CHitosan: manufacture, properties, and usage. Nova Science Publishers, Inc, New York
- Fan W, Yan W, Xu Z, Ni H (2012) Biointerfaces Formation mechanism of monodisperse, low molecular weight chitosan nanoparticles by ionic gelation technique. *Colloids Surf B Biointerfaces* 90:21–27. <https://doi.org/10.1016/j.colsurfb.2011.09.042>
- Dmour I, Taha MO (2017) Novel nanoparticles based on chitosan-dicarboxylate conjugates via tandem ionotropic/covalent crosslinking with tripolyphosphate and subsequent evaluation as drug delivery vehicles (B). *Int J Pharm* 529:15–31. <https://doi.org/10.1016/j.ijpharm.2017.06.061>
- Alves HJ, Furman M, Kugelmeier CL et al (2017) Effect of shrimp shells milling on the molar mass of chitosan. *Polímeros* 27:41–47
- Delezuk JA, de M, Cardoso, Domard MB, Campana-Filho A SP (2011) Ultrasound-assisted deacetylation of beta-chitin: Influence of processing parameters. *Polym Int* 60:903–909. <https://doi.org/10.1002/pi.3037>
- Mohammadi A, Hashemi M, Masoud Hosseini S (2016) Effect of chitosan molecular weight as micro and nanoparticles on antibacterial activity against some soft rot pathogenic bacteria. *LWT - Food Sci Technol* 71:347–355. <https://doi.org/10.1016/j.lwt.2016.04.010>
- Vasilieva T, Sigarev A, Kosyakov D et al (2017) Formation of low molecular weight oligomers from chitin and chitosan stimulated by plasma-assisted processes. *Carbohydr Polym* 163:54–61. <https://doi.org/10.1016/j.carbpol.2017.01.026>
- No HK, Nah JW, Meyers SP (2002) Effect of time/temperature treatment parameters on depolymerization of chitosan. *J Appl Polym Sci* 87:1890–1894
- San Juan A, Montembault A, Gillet D et al (2012) Degradation of chitosan-based materials after different sterilization treatments. In: 6th EEIGM international conference on advanced materials research, pp 1–5
- Yue W (2014) Prevention of browning of depolymerized chitosan obtained by gamma irradiation. *Carbohydr Polym* 101:857–863. <https://doi.org/10.1016/j.carbpol.2013.10.011>
- Jung J, Zhao Y (2011) Characteristics of deacetylation and depolymerization of β -chitin from jumbo squid (*Dosidicus gigas*) pens. *Carbohydr Res* 346:1876–1884. <https://doi.org/10.1016/j.carres.2011.05.021>
- Pan AD, Zeng HY, Foua GB et al (2016) Enzymolysis of chitosan by papain and its kinetics. *Carbohydr Polym* 135:199–206. <https://doi.org/10.1016/j.carbpol.2015.08.052>
- Dziril M, Grib H, Laribi-Habchi H et al (2015) Chitin oligomers and monomers production by coupling γ radiation and enzymatic hydrolysis. *J Ind Eng Chem* 26:396–401. <https://doi.org/10.1016/j.jiec.2014.12.015>
- Tsao CT, Chang CH, Lin YY et al (2011) Kinetic study of acid depolymerization of chitosan and effects of low molecular weight chitosan on erythrocyte rouleaux formation t. *Carbohydr Res* 346:94–102. <https://doi.org/10.1016/j.carres.2010.10.010>

27. Tian F, Liu Y, Hu K, Zhao B (2004) Study of the depolymerization behavior of chitosan by hydrogen peroxide. *Carbohydr Polym* 57:31–37. <https://doi.org/10.1016/j.carbpol.2004.03.016>

28. Alves HJ, Arantes MK, Muniz GIB, Ellendersen LSN (2017) Patente: Privilégio de Inovação. Número do registro: BR102017022250: “Processamento de exoesqueleto de crustáceos para obtenção de nanoquitosana”, Instituição de registro: INPI - Instituto Nacional da Propriedade Industrial, Depósito: 16/10/2017, Brasil, 2017

29. Kasai MR (2007) Calculation of Mark–Houwink–Sakurada (MHS) equation viscometric constants for chitosan in any solvent–temperature system using experimental reported viscometric constants data. *Carbohydr Polym* 68:477–488. <https://doi.org/10.1016/j.carbpol.2006.11.006>

30. Santos ZM, Caroni ALPF., Pereira MR et al (2009) Determination of deacetylation degree of chitosan: a comparison between conductometric titration and CHN elemental analysis. *Carbohydr Res* 344:2591–2595. <https://doi.org/10.1016/j.carres.2009.08.030>

31. Berne BJ, Pecora R (2000) Dynamic light scattering: with applications to chemistry, biology, and physics. Wiley, New York

32. Pecora R (2000) Dynamic light scattering measurement of nanometer particles in liquids. *J Nanoparticle Res* 2:123–131

33. Mao S, Shuai X, Unger F et al (2004) The depolymerization of chitosan: effects on physicochemical and biological properties. *Int J Pharm* 281:45–54. <https://doi.org/10.1016/j.ijpharm.2004.05.019>

34. Choi W-S, Ahn K-J, Lee D-W et al (2002) Preparation of chitosan oligomer by irradiation. *Polymer Degrad Stab* 78:533–538

35. Jia Z, Shen D (2002) Effect of reaction temperature and reaction time on the preparation of low-molecular-weight chitosan using phosphoric acid. *Carbohydr Polym* 49:393–396. [https://doi.org/10.1016/S0144-8617\(02\)00026-7](https://doi.org/10.1016/S0144-8617(02)00026-7)

36. Czechowska-Biskup R, Rokita B, Lotfy S et al (2005) Degradation of chitosan and starch by 360-kHz ultrasound. *Carbohydr Polym* 60:175–184. <https://doi.org/10.1016/j.carbpol.2004.12.001>

37. Zhou HY, Chen XG, Kong M et al (2008) Effect of molecular weight and degree of chitosan deacetylation on the preparation and characteristics of chitosan thermosensitive hydrogel as a delivery system. *Carbohydr Polym* 73:265–273. <https://doi.org/10.1016/j.carbpol.2007.11.026>

38. Zhang W, Zhang J, Jiang Q, Xia W (2012) Physicochemical and structural characteristics of chitosan nanopowders prepared by ultrafine milling. *Carbohydr Polym* 87:309–313. <https://doi.org/10.1016/j.carbpol.2011.07.057>

39. Zainol I, Akil HM, Mastor A (2009) Effect of γ -irradiation on the physical and mechanical properties of chitosan powder. *Mater Sci Eng C* 29:292–297. <https://doi.org/10.1016/j.msec.2008.06.026>

40. Kasai MR, Arul J, Charlet G (2008) Fragmentation of chitosan by ultrasonic irradiation. *Ultrason Sonochem* 15:1001–1008. <https://doi.org/10.1016/j.ultsonch.2008.04.005>

41. Luo WB, Han Z, Zeng XA et al (2010) Study on the degradation of chitosan by pulsed electric fields treatment. *Innov Food Sci Emerg Technol* 11:587–591. <https://doi.org/10.1016/j.ifset.2010.04.002>

42. Zhang W, Zhang J, Xia W (2014) Effect of ball-milling treatment on physicochemical and structural properties of chitosan. *Int J Food Prop* 17:26–37. <https://doi.org/10.1080/10942912.2011.608175>

43. Lim LY, Khor E, Ling CE (1999) Effects of dry heat and saturated steam on the physical properties of chitosan. *J Biomed Mater Res* 48:111–116

44. Tsaih ML, Chen RH (2003) The effect of reaction time and temperature during heterogenous alkali deacetylation on degree of deacetylation and molecular weight of resulting chitosan. *J Appl Polym Sci* 88:2917–2923. <https://doi.org/10.1002/app.11986>

45. Gomes LP, Andrade CT, Silva JT et al (2014) Green synthesis and physical and chemical characterization of chitosans with a high degree of deacetylation, produced by a binary enzyme system. *J Life Sci* 8:276–282